

Case Report

Malignant transformation of benign thyroid nodule is caused by prolonged H₂O₂ insult that interfered with the STAT3 pathway?

Ching Chin Lee¹, Mardiaty Iryani Abdullah¹, Sarni Mat Junit¹, Khoon Leong Ng², Sing Ying Wong¹, Nur Siti Fatimah Ramli¹, Onn Haji Hashim^{1,3}

¹Department of Molecular Medicine, ²Department of Surgery, ³University of Malaya Centre for Proteomics Research, Faculty of Medicine, University of Malaya, Kuala Lumpur, Malaysia

Received February 23, 2016; Accepted June 4, 2016; Epub September 15, 2016; Published September 30, 2016

Abstract: Background: Approximately 60% of papillary thyroid cancer (PTC) cases in Malaysia occur as a result of long-standing benign thyroid nodules. However, the underlying mechanisms that led to the malignant transformation are not understood. Methods & Results: Here, we report a study of benign and malignant thyroid tissues of a Malay woman presented with concurrent benign thyroid cyst and PTC. The same patient had only presented with neck swelling five years earlier. Whole-exome capture sequencing of extracted DNA from the PTC tissue revealed mutations of 1799 T>A (p.V600E) and c.353 G>A (p.R118Q) in the V-Raf Murine Sarcoma Viral Oncogene Homolog B (*BRAF*) and the Thyrotropin-Releasing Hormone (*TRH*) genes, respectively. When the benign cyst of the patient was subjected to direct PCR screening for both the mutations, only the c.353G>A mutation of the *TRH* gene was detected. Both the benign and malignant tissues also showed decrease or loss of expression of multiple iodide metabolism genes with elevated *BRAF* expression. Analyses by 2-dimensional electrophoresis and Ingenuity Pathway algorithm indicated “reactive oxygen species insult”, “tissue injury/inflammation”, “cell proliferation” and “apoptosis and necrosis inhibitions” in the benign cyst. Both the benign and PTC tissues demonstrated different expression patterns of activated signal transducer and activator of transcription 3 (pY-STAT3), with the former tissue expressing a novel putative STAT3 isoform termed STAT3ε. Discussion: The data of our study, when taken together, appear to suggest that prolonged H₂O₂ insults in the patient might have resulted in extreme oxidative stress that interfered with the MAPK and STAT3 pathways, which then led to *BRAF*^{V600E} mutation and consequential loss of function of p53 as well as the altered metabolisms and malignant transformation that occurred in PTC.

Keywords: Benign thyroid cyst, papillary thyroid cancer, *BRAF*^{V600E}, *TRH* gene, H₂O₂, STAT3 and tumorigenesis

Introduction

Enlargement of the thyroid gland such as a thyroid nodule or a goiter is a common endocrine problem. Whilst palpable thyroid nodules have been reported in 4-7% of the population [1, 2], the actual prevalence of thyroid nodules detected by ultrasonography in some areas can be as high as 67% [3, 4]. In general, women are more susceptible to thyroid problems than men [5, 6], with the incident rate increasing with age for thyroid nodules or goiter [7, 8].

Goiters can be classified into euthyroid (simple goiter), hyperthyroid (toxic nodular goiter or Grave's disease) or hypothyroid (iodine deficiency, congenital hypothyroidism or Hashimoto's thyroiditis) according to the functional sta-

tus of the gland. Goiter due to Grave's disease is characteristically associated with a diffusely enlarged gland with a smooth surface and often with a bruit. A diffuse, smooth goiter with negative anti-thyroid antibodies may be due to iodine deficiency. In this case, the thyroid gland enlarges as it attempts to comply with the pituitary's demand. Other thyroid problems such as congenital hypothyroidism and other inflammatory conditions in the thyroid gland are also responsible for the formation of goiter. A nodular thyroid gland with hypothyroidism and positive anti-thyroid antibodies is suggestive of Hashimoto's thyroiditis [9, 10].

Despite that goiters such as follicular adenoma, colloid nodules, benign cysts or nodular thyroiditis are usually presented in benign

Malignant transformation of thyroid cyst

Table 1. Summary of detected nucleotide variants (SNP & InDels) of the 32 candidate genes in the patient

Gene	Nucleotide(s) Alterations							
TG	rs180223	rs2069550	rs16904774	rs16893332	rs853326	rs2069568	rs56541861	rs1133076
PAX8								
NKX2-1								
EGF	rs2237051	rs4698803	*rs79786166					
KISS1R	rs350132							
PIK3CA								
CDKN1A								
RASSF1								
BRAF	rs9648696	**rs113488022						
CALCA	rs5239							
PPARG	rs13306747							
HRAS	rs12628							
TPO	rs2280132	rs2175977	rs1126797	rs732608	rs732609	rs1126799		
RET	rs1800860							
NRAS								
TRH	**NM_007117: c.G353A: p.R118Q	rs5662	rs5663					
TSHR	rs3783942	rs3783941	rs1991517					
SLC26A4								
KRT19	rs4601	rs4602	rs11550883					
ADCT10	rs203795	rs2071921						
LGALS3								
LGALS3BP	rs3744166							
KRT10	rs42611597							
BGLAP	rs1052053	rs1052067						
GNAS	rs74897360	rs7121						
SERPINA7	rs1804495							
CTNNA1								
TIMP3	rs9862	rs11547635						
KRAS	rs4362222							
PTEN	*rs71022512							
TP53	rs1042522							
CCDC6	rs1053265	rs1053266	rs1171830	rs77152637				

*InDels. **Mutation (SIFT score of <0.05; PolyPhen-2 score of >0.85. Grey: Homozygous.

forms, 7-17% cases have been shown to be cancerous [11-14]. Presence of nodules in young males is indicative of higher risk of thyroid cancer, while toxic and non-toxic nodular goiters are more prone to undergo malignant transformation when compared to Grave's disease [15]. In addition, a study carried out in Hospital University Sains Malaysia (HUSM) from years 1994 to 2004 has shown that 60% of thyroid cancers that were detected occurred with a background of prolonged goiter [16]. In view of the increased risk of the Malaysian goitrous patients developing into thyroid cancer, we examined a case of concurrent benign thyroid cyst and papillary thyroid cancer, aiming to elucidate the molecular mechanisms underlying tumorigenesis of a long-standing thyroid nodule.

Subject, materials and methods

Case

A 53-year-old woman, who presented with anterior neck swelling at 48 years of age, complained of palpitations and sweating but without any compressive or obstructive symptoms. The patient was clinically euthyroid with TSH of 2.65 mU/L and free T₄ of 14.9 pmol/L. Ultrasound scan of the neck showed a 3.9 x 2.7 x 4.9 cm nodule with increased vascularity and a 0.3 x 0.2 x 0.3 cm cyst on the left and right lobes of the thyroid gland, respectively. Fine needle aspiration of the left thyroid nodule showed suspicion for cancer (Bethesda classification V) and histopathologic examination (HPE) of surgical material obtained during a left hemithyroidectomy confirmed for PTC. The HPE

Malignant transformation of thyroid cyst

revealed an encapsulated lesion composed of malignant cells arranged in papillary and follicular patterns. These neoplastic cells were vesicular and mildly pleomorphic, and exhibited nuclear overlapping with occasional optically-clear nuclei and nuclear inclusions. Some of the cells also exhibited central nuclear grooves. However, psammoma bodies, which are commonly seen in PTC cases, were not detected in the cells. When right hemi thyroidectomy was done after one month, no evidence of malignancy was shown by HPE. Whole body scan (WBS) performed on 9 and 22 months after the thyroidectomy showed no evidence of residual or metastatic functioning papillary carcinoma of thyroid. This study and its written consent procedure were approved by the University of Malaya Medical Centre (UMMC) Ethical Committee (Institutional Review Board) in accordance with the ICH-GCP guideline and the Declaration of Helsinki (Reference number, 925.8).

Thyroid tissue samples

Thyroid tissue specimens obtained during the thyroidectomy were immediately stored in the Allprotect Tissue Reagent® Qiagen until further processing. Genomic DNA, RNA and protein were extracted simultaneously from the patient's thyroid tissue samples using Qiagen AllPrep DNA/RNA/Protein mini kit according to the manufacturer's protocol.

Whole-exome sequencing and mutation analyses

Whole-exome capture sequencing was performed on the extracted DNA from the PTC tissue with 90 bp-paired end reads by Illumina HiSeq 2000 platform. Raw image data and base calling were processed using Illumina Pipeline software version 1.7 with the default parameters. Bioinformatics analyses were carried out using Burrows-Wheeler Aligner (BWA) for mapping reads [17], SOAPsnp [18], SAMtools [19] and SOAPsv (<http://soap.genomics.org.cn/SOAPsv.html>) for single nucleotide variation (SNV), small insertions and deletions (InDels) and structure variation (SV) detections, respectively. Mutation screening was performed on 32 candidate genes associated with goiter development, thyroid hormone signaling and thyroid cancers (Table 1). Variants detected within intergenic and intronic regions were

excluded except for those in areas close to the 3' and 5' splice junctions (maximum 20 nt upstream of the 3' and 5' splice-sites). Other variants were filtered and examined for their clinical impact based on four databases, namely the NCBI dbSNP132 (http://www.ncbi.nlm.nih.gov/projects/SNP/snp_summary.cgi?build_id=132), SNPedia (<http://www.snpedia.com/index.php/SNPedia>), ExAC browser (<http://exac.broadinstitute.org>) and Ensembl (<http://www.ensembl.org/info/genome/variation/index.html>). The effects of the variants on protein function were predicted using SIFT (<http://sift.bii.a-star.edu.sg/>) and PolyPhen-2 (<http://genetics.bwh.harvard.edu/pph2/index.shtml>). A SIFT score of <0.05 indicates "damaging" whereas PolyPhen-2 scores of >0.85 indicates "probably damaging" effect. Any variant predicted to be damaging were further screened in the DNA extracted from the benign cyst tissue using PCR-direct sequencing method [20]. For the SV data analysis, genes with alterations in the exonic and 5'/3' untranslated regions were annotated using IPA software to determine its biological functions and pathways involved. The biological relationships between the affected genes and the 32 candidate genes included in the initial screening were also investigated. Variants which showed connection with the 32 candidate genes were examined through "Database of Genetic Variants" (<http://dgv.tcag.ca/dgv/app/home?ref=GRCh37/hg19>).

Quantitative real-time polymerase chain reaction (qRT-PCR) analysis for BRAF and iodide metabolism genes

Expression of *BRAF* and four iodide metabolism genes including Thyroid Hormone Receptor (*TSHR*), Thyroid Peroxidase (*TPO*), Thyroglobulin (*TG*) and Sodium-iodide symporter (*NIS*) were compared between the two tissues using qRT-PCR. One µg of tcRNA extracted from the benign cystor PTC tissue was converted to complementary DNA (cDNA) using High Capacity RNA-to-cDNA kit (Applied Biosystems, USA). Quantitative PCR was carried out using the StepOne Real-Time PCR System (Applied Biosystems, USA) with 40 amplification cycles. Melting curve analyses were performed for all primers to ensure single amplification product. The list of primers is shown in Table 2. Each reaction consisted 10 ng of cDNA, 0.2 mM forward and reverse primers, 2X Fast SYBR® Green Master Mix (Applied Biosystems, USA) in a final volume

Malignant transformation of thyroid cyst

Table 2. Sequences of the primers used for quantitative real-time PCR analysis

Genes	Exon	Primer Sequence	Fragment size (bp)	Annealing temperature (°C)
<i>TBP</i>	4	Forward 5' CACGAACCACGGCACTGATT 3'	89	59
	5	Reverse 5' TTTTCTTGCTGCCAGTCTGGAC 3'		
<i>BRAF</i>	15	Forward 5' GAGTGGGTCCCATCAGTTTG 3'	181	59
	15	Reverse 5' CTGGTCCCTGTTGTTGATGTT 3'		
<i>TG</i>	31-32	Forward 5' CCGGAAGAAAGTTATACTGGAAG 3'	356	59
	34-35	Reverse 5' TTTGAGCAATGGGCTTCTG 3'		
<i>TSHR</i>	4-5	Forward 5' CCTCCTAAAGTTCCTTGGCATT 3'	243	59
	7-8	Reverse 5' AGGTAAACAGCATCCAGCTTTG 3'		
<i>NIS</i>	1-2	Forward 5' CACCAGCACCTACGAGTACC 3'	143	59
	3-4	Reverse 5' CCCGGTCACTTGGTTCAG 3'		
<i>TPO</i>	4	Forward 5' TCCAAACTTCTGAGCCAA 3'	241	59
	5	Reverse 5' CTCCTGTGATGGCCTGTAT 3'		

of 20 μ L. All qRT-PCR experiments were performed in triplicates. Gene expressions were normalised against *TATA-box binding protein* (TBP), a housekeeping gene. The experiment was repeated by comparing both the tissues with another 3 control thyroid tissues (benign).

2-DE analysis

One hundred μ g of cell lysate proteins from both benign cyst and PTC tissues were reconstituted in rehydration solution containing 7 M urea, 2 M thiourea, 2% w/v CHAPS, 0.5% v/v IPG buffer, orange G, 0.07 mg DTT and protease inhibitor for 30 mins. The reconstituted protein samples were then incubated with an immobiline pH gradient strip (13 cm, non-linear, pH 4-7, GE Healthcare, Uppsala, Sweden) for 18 hrs at room temperature. The first dimension separation was performed using an Ettan IPGphor III (GE, Uppsala, Sweden) ran at the following four parameter setting steps: 1) 500 V, 1 hr, step and hold; 2) 1000 V, 1 hr, gradient; 3) 8000 V, 2 hrs 30 mins, gradient and 4) 8000 V, 2 hrs 30 mins, step and hold. The strips were subsequently incubated in SDS equilibration buffer containing 1% w/v dithiothreitol (DTT) for 20 mins, followed by a second equilibration using the same buffer containing 4.5% w/v iodoacetamide instead of DTT for another 20 mins. The equilibrated strips were then subjected to second dimension separation in a 8-13% gradient polyacrylamide gel using the SE 600 Ruby electrophoresis system (GE Healthcare, Uppsala, Sweden) at a constant voltage of 50 V and 40 mA/gel for 40 min, and then switched to 600 V and 40 mA/gel until the bromophenol blue marker was 1 mm away from the bottom

of the gel. Each tissue sample was subjected to the same procedure for at least 3 times (triplicated).

Image and data analyses

Silver stained 2-DE gels were scanned using the ImageScanner III (GE Healthcare, Uppsala, Sweden). Protein profiles were compared between the benign and malignant tissues using the Image Master Platinum 7.0 software (GE Healthcare). Briefly, protein spots were normalized using root-mean-square deviation (RMSD) to minimize variations between gels of the same tissue for the comparison of protein abundance between the tissues. Statistical analysis was performed by one way ANOVA using Image Master Platinum 7.0 software. The test was conducted on the normalized values from both benign and PTC groups. Only protein spots with fold difference >1.5 and statistically significance, $P \leq 0.01$, were considered to have significantly changed in abundance.

In-gel tryptic digestion and MALDI-TOF/TOF mass spectrometry analysis

Protein spots of altered abundance were excised manually from 2-DE gels according to a published protocol [21] and analyzed using 6520 Accurate-Mass Q-TOF LC/MS system (Agilent, Santa Clara, CA, USA). Briefly, digested samples were first reconstituted in 5 μ L of the initial LC mobile phase (0.1% formic acid) before injected into the Nano-flow LC 1200 series (Agilent, Santa Clara, CA, USA). Digested peptides were enriched using an enrichment column and then separated on an HPLC Chip-

Malignant transformation of thyroid cyst

Protein column (C18 reverse phase, 300 Å, 43 mm, Agilent, Santa Clara, CA, USA) with a 3%-50% linear gradient of solvent B (90% Acetonitrile and 0.1% Formic acid) for 30 min with a flow rate of 0.3 µL/min. Mass Hunter Qual acquisition software (Agilent, Santa Clara, CA, USA) was used to acquire the mass spectra (8 masses per second from 115 to 3000 *m/z*) followed by collision-induced dissociation of the four most intensive ions. MS/MS data were acquired in the range of 50-3000 *m/z*.

Database search

Data analysis was carried out using the Spectrum Mill software (Agilent, Santa Clara, CA, USA) and database search using the Swiss-Prot mammalian database. Mass-tolerance of precursor and product ions was set to ± 20 and ± 50 ppm, respectively. Meanwhile, carbamidomethylation of cysteine was set as fixed modification and methionine oxidation was set as variable modifications. A protein was considered identified when the score was higher than 20, peptide mass error less than 5 ppm, forward-reverse score more than 2, peptide score more than 6 and Scored Peak Intensity (SPI%) more than 60 percent.

IPA

The identified proteins were analyzed algorithmically using Ingenuity Pathways Analysis (IPA, <http://www.ingenuity.com>) software to generate a set of interactive networks taking into consideration of canonical pathways, relevant biological interactions as well as cellular and disease processes based on the information contained in the Ingenuity Knowledge Base. A Right-tailed Fischer's exact test was used to calculate a *p*-value indicating the likelihood of focused genes to belong to a network versus those obtained by chance. The IPA system computes a score (Z-Score) to infer the activation status of predicted transcriptional regulators. A score ≥ 2.0 indicates significantly "activation" whereas ≤ 2.0 indicates significantly inhibition.

Quantitative western blot analysis of STAT3 phosphorylation (pY705)

Approximately 20 µg protein sample of benign cyst and PTC tissues were separated by electrophoresis in a 12% sodium dodecyl sulfate polyacrylamide gel. The separated proteins

were later transferred onto a polyvinylidene difluoride (PVDF) membrane. Western blot analysis was performed using rabbit monoclonal EP2147Y primary antibody (Abcam Cat# ab76315, RRID: AB_1658549, 1:2000) [22] and WesternDot 625 Western blot kits (Invitrogen, USA) to detect the presence of phosphorylated STAT3 (pY-STAT3) protein in the tissue specimens from areas. The expression of pY-STAT3 in benign and malignant tissues was quantitated by densitometry scanning using Image-J software (<http://rsbweb.nih.gov/ij/>) and normalized to the expression of beta-actin (Abcam Cat# ab8227, RRID: AB_2305186, 1:2000) [23]. The ratio of STAT3 variants in the benign cyst was also compared to that of the PTC.

Search of alternatively spliced STAT3 mRNA transcript

Complimentary DNA samples obtained from tcRNA-cDNA conversion were used as template to PCR-amplify the STAT3 using a pair of primers, forward 5'cttgacacacgggtacctgga 3' and reverse 5'cactccgagggtcaactccat 3' that cover a region from c.28 to c.2275 in transcript variant 1 (NM_139276.2). PCR amplification was performed as previously described [24].

Results

Mutation screening

Whole-exome sequencing of DNA extracted from the PTC tissue generated approximately 63 million of clean read, which covered 99.7% of the targeted region with a mean depth of 70.81X. SOAPsnp and InDels analyses revealed a total of 51 variants in the exonic and flanking intronic regions (maximum 20 nt upstream of the 3' and 5' splice-sites) of the 31 candidate genes (**Table 1**). Amongst these alterations, c.353G>A (p.R118Q) and c.1799T>C (p.V600E), which are respectively located at the *TRH* and *BRAF* genes, were predicted as "deleterious mutations" by PolyPhen-2 and SIFT. However, only the c.353G>A mutation of the *TRH* gene (**Figure 1**) was detected when the benign cyst was subjected to direct PCR screening for the two mutations. Chromosomal abnormalities detected across exonic, splicing and 5'UTR regions of 9 genes in the PTC tissue included *FLG*, *OR52N1*, *OVCH2*, *TDG*, *LOC100507642*, *FADS6*, *AURKA*, *LNP1* and *INTS1*. Molecular

Malignant transformation of thyroid cyst

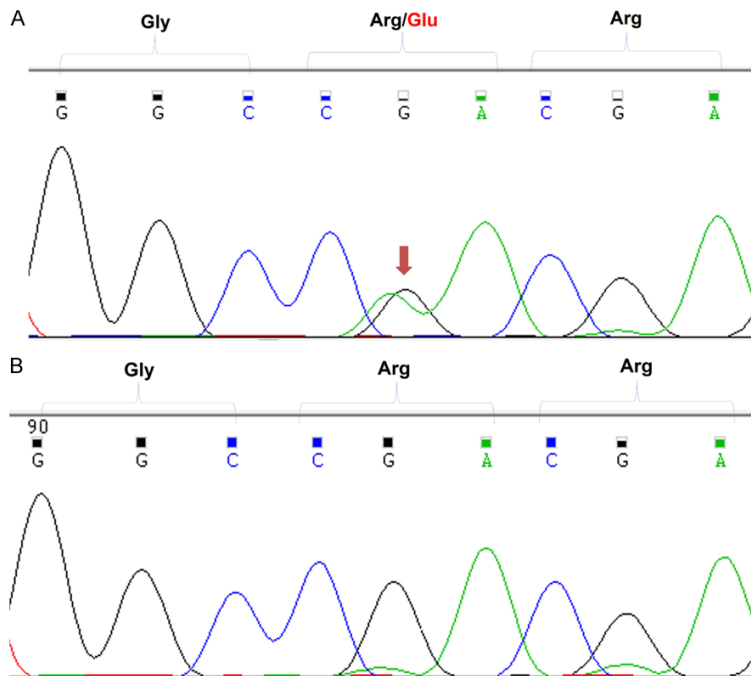


Figure 1. DNA sequencing profiles. Electropherogram profiles of the c.353G>A (p.R118Q) mutation (A) and a wild type (WT) allele (B). Red arrow indicates the nucleotide transition in the *TRH* gene.

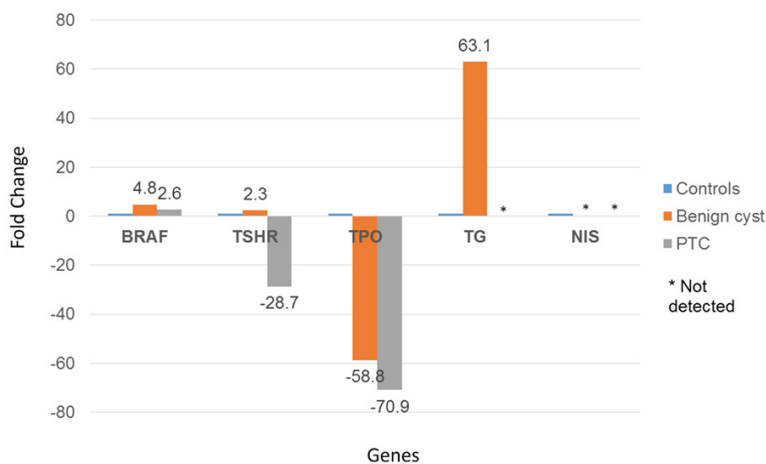


Figure 2. Real time PCR analysis. Expression of *NIS* was not detected in both benign cyst and PTC tissue whereas expression of *TG* was not detected in the PTC tissue. Comparison of *BRAF*, *TSHR* and *TPO* genes expression between benign cyst, PTC and controls 1, 2 and 3.

network analysis of the genes using IPA software showed direct connections between *AURKA* and the *RASSF1/HRAS* genes and the association of *TDG* with *HRAS/NKX2-1* genes. Search of the two chromosomal abnormalities against Database of Genomic Variants (DGV, <http://dgv.tcag.ca/dgv/app/home>) revealed deletion dgv197e201, chr12: 104379506-

104389726 in the *TDG* gene in 81 out of 96 Southeast Asian Malays [25]. Meanwhile, the insertion esv3402144, chr20:54963150-54963210 in *AURKA* gene was reported in 3/185 individuals under the 1000 Genomes Project Consortium project [26].

Expression of *BRAF*, *TSH-R*, *TPO*, *TG* and *NIS* genes

In this experiment, the transcript levels of selective genes in the benign cyst, PTC lesion and three control tissues were measured by qRT-PCR and expression of the target genes was normalized to the expression of the *TBP* gene. Our results showed that the *NIS* transcript was not detected in both benign and PTC tissues. Whilst *TG* was also not expressed in the PTC tissue, enhanced expression of *TG* relative to the controls was detected in the benign cyst. The expression of *BRAF* and *TSHR* genes was relatively higher in the benign tissue compared to that of PTC. When compared with the three *BRAF*^{V600E} mutation-free control tissues, the benign cyst showed high expression of all the selected genes except *TPO*. However, only the expression of the *BRAF* gene in the PTC tissue was higher than that of the three control tissues (Figure 2).

2-DE and identification of differentially expressed proteins

Figure 3 shows representative protein profiles of the benign thyroid cyst and PTC tissues when analysed by 2-DE. Each tissue was analysed in triplicate to ensure reproducibility. Image analysis of silver stained gels showed an average of 670 ± 62 and 668 ± 16 spots from the benign cyst and PTC tissues, respectively. Only spots that appeared in all gel images from each tis-

Malignant transformation of thyroid cyst

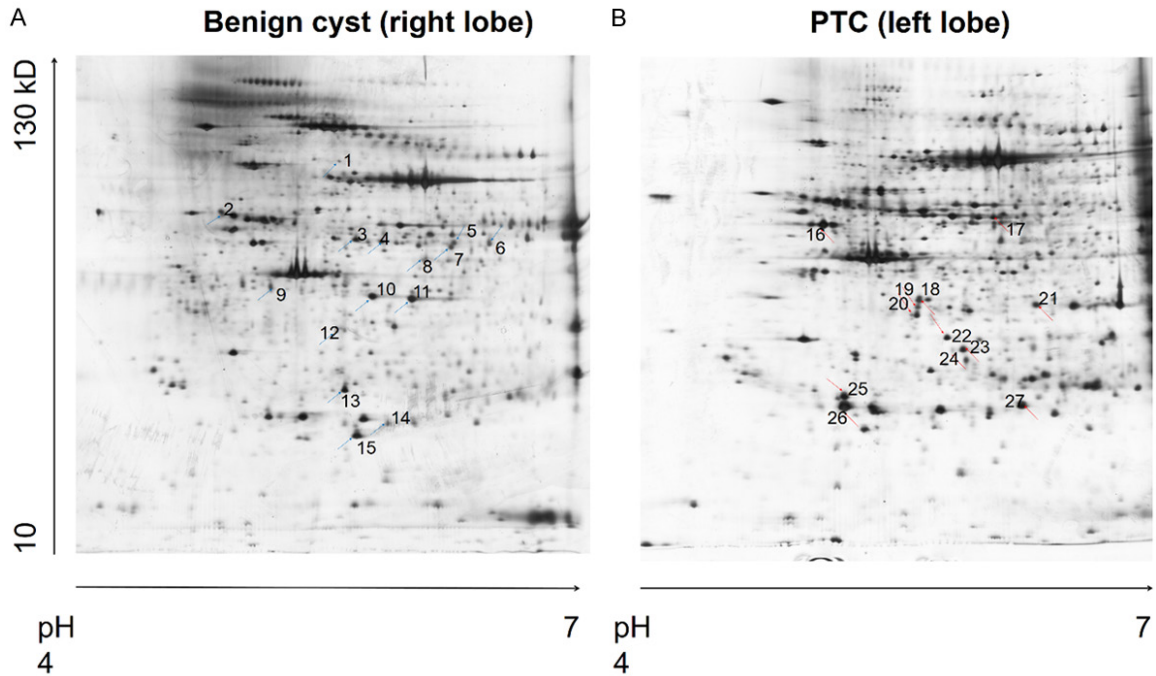


Figure 3. Representative 2-DE maps of benign thyroid cyst and PTC tissue. Figure demonstrates 2-DE maps of benign thyroid cyst (A) and PTC tissue (B) from the same patient. The proteins were separated on a pH 4-7 nonlinear IPG strip, followed by a 8-15% SDS-polyacrylamide gel. The gel was silver-stained and spots of altered abundance (indicated by arrows) were analyzed by MALDI-TOF/TOF mass spectrometry.

sue were compared and subjected to statistical analysis ($P < 0.01$). Quantitative analysis of the 2-DE gels revealed 27 proteins spots with more than 1.5 fold changes between the two tissues. Twenty-three of the spots, which comprised 21 proteins, were subsequently identified by tandem mass spectrometry (MS/MS) and database query (**Table 3**).

Pathway interactions and biological process analysis

Analysis of the 21 proteins using IPA identified two associated “cancer, endocrine system disorders, organismal injury and abnormalities” (**Figure 4A**) and “amino acid metabolism, small molecule biochemistry, nucleic acid metabolism” networks (**Figure 4B**), with scores of 44 and 10, respectively. A score of 2 or higher indicates at least a 99% confidence of not being generated by random chance and higher scores indicate a greater confidence. Cancer related signalling pathways such as p38/ERK 1/2 MAPK, PKC(s) and Akt/NF- κ B pathways were shown in the “cancer, endocrine system disorders, organismal injury and abnormalities” network.

Canonical pathway analysis ranked the “acute phase response signalling” at the top with the highest significance ($P < 6.85 \times 10^{-07}$) and indicated that this pathway was “activated” (Z-score: 2) in the benign tissue. Other pathways, namely “coagulation system”, “extrinsic prothrombin activation pathway”, “intrinsic prothrombin activation pathway” and “G-protein signaling mediated by Tubby protein”, were particularly relevant to the data set but the activity patterns of these pathways were not available. The five top-most predicted activated upstream regulators by z-score for the data set (using benign tissue as reference) were fenofibrate, PPARA, HRAS, D-glucose and nitrofurantoin. However, none of these regulators was significantly “activated” (z-score ≥ 2.0) in the PTC tissue. In contrast, the five most predicted inhibited upstream regulators were PD98059, STAT3, L-triiodothyronine, MYC and TP53. IL-6 was ranked behind TP53 with a score of -1.341. Amongst these regulators, only PD98059 was significantly “inhibited” in the PTC tissue with a score of less than -2. However, STAT3 was shown to be significantly activated (z-score ≥ 2.0) when cancer tissue was used as a reference gel in the comparison (**Table 4A**).

Malignant transformation of thyroid cyst

Table 3. List of proteins with differential abundance identified by LC MS/MS Q-TOF

Spot No	Anova	Fold Ratio	Protein name	Swiss-Prot accession no.	Mw (kDa)	Theoretical pl	Distinct MS/MS Search Score	Summed	No. of matched peptides	% of sequence coverage
1	<0.001	6.50942	Acylamino-acid-releasing enzyme (APEH)	P13798	82.193	5.29	40.83		3	4
2	<0.001	2.32927	Alpha-1-antitrypsin (SERPINA1)	P01009	46906.8	5.37	125.07		9	28.7
3	<0.001	2.82044	Fibrinogen gamma chain (FGG)	P02679	52.1383	5.37	179.45		11	26.9
4	0.005	7.60295	Fibrinogen gamma chain (FGG)	P02679	52.1383	5.37	57.96		4	7.9
7	<0.001	13.5747	4-trimethylaminobutyraldehyde dehydrogenase (ALDH9A1)	P49189	54.7138	5.69	65.03		5	9.7
8	0.003	1.67731	26S protease regulatory subunit 7 (PSMC2)	P35998	49.0324	5.71	102		7	17.3
9	0.006	6.5896	Haptoglobin (HP)	P00738	45.8891	6.13	104.06		6	15.5
10	<0.001	10.4851	Fibrinogen beta chain (FGB)	P02675	56611.8	8.54	275.42		17	40.9
11	<0.001	14.4785	Fibrinogen beta chain (FGB)	P02675	56611.8	8.54	160.33		11	27.4
12	0.001	2.50237	Guanine nucleotide-binding protein G(I)/G(S)/G(T) subunit beta-2 (GNB2)	P62879	38072.1	5.6	127.22		8	25.2
13	0.003	7.01605	Prohibitin (PHB)	P35232	29.8606	5.57	106.16		7	26.4
14	0.009	3.90298	Thioredoxin-dependent peroxide reductase, mitochondrial (PRDX3)	P30048	28034.5	7.68	45.89		4	15.6
15	0.002	5.84935	Peroxiredoxin-2 (PRDX2)	P32119	22062.7	5.66	126.14		8	36.8
16	0.009	2.30989	ATP synthase subunit beta, mitochondrial (ATP5B)	P06576	56558.9	5.26	311.99		17	40.2
17	0.003	2.01754	Selenium-binding protein 1 (SELENBP1)	Q13228	52960.5	5.93	150.42		10	25.4
18	0.002	5.06965	Actin, cytoplasmic 2 (ACTG1)	P63261	42134.4	5.31	57.41		4	9.8
20	<0.01	2.84281	Guanine nucleotide-binding protein G(I)/G(S)/G(T) subunit beta-1 (GNB1)	P62873	38175.1	5.6	98.75		6	22.3
21	0.003	12.1073	Annexin A1 (ANXA1)	P04083	38941.8	6.57	21.86		2	4.9
22	0.002	2.30797	Annexin A3 (ANXA3)	P12429	36545.8	5.62	206.29		13	23.2
23	0.001	3.85539	3-hydroxyisobutyrate dehydrogenase, mitochondrial (HIBADH)	P31937	35727.7	8.38	58.97		4	17.2
24	0.005	1.91072	F-actin-capping protein subunit beta (CAPZB)	P47756	31635.2	5.36	67.03		4	16.2
25	0.007	9.79335	Cathepsin B (CTSB)	P07858	38790.8	5.88	67.75		4	14.7
26	0.007	2.72695	Apolipoprotein A-I (APOA1)	P02647	38790.8	5.56	117.35		7	28.8

Malignant transformation of thyroid cyst

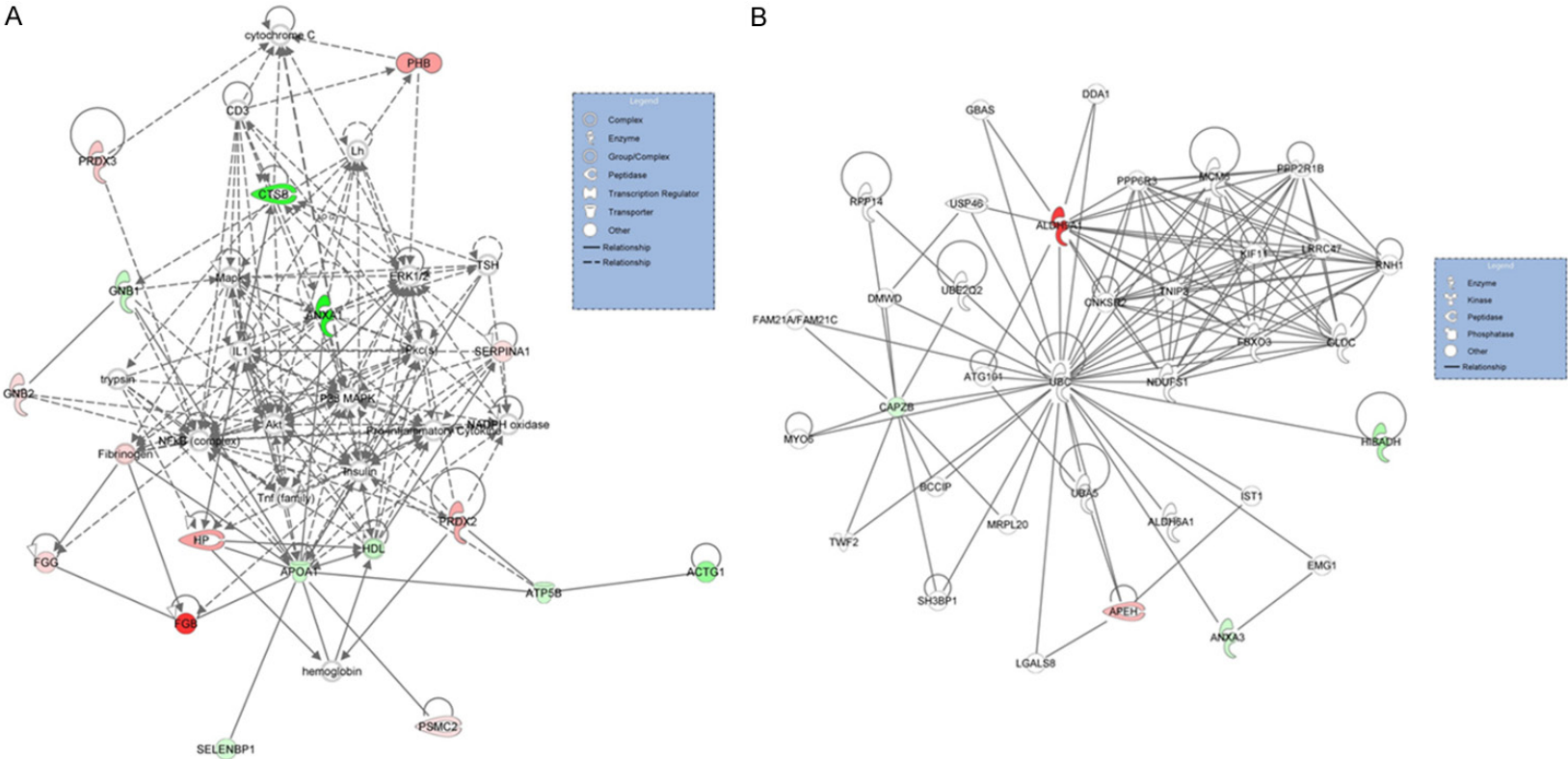


Figure 4. IPA graphical representation of the molecular relationships in “cancer, endocrine system disorders, organismal injury and abnormalities” network (A) and “amino acid metabolism, small molecule biochemistry, nuclei acid metabolism” network (B) in benign cyst vs PTC tissues. Each network is displayed graphically as nodes (genes) and edges (the biological relationships between the nodes). Nodes in red indicate up-regulated genes while those in green represent down-regulated genes. Nodes without colours indicate unaltered expression. Various shapes of the nodes represent the functional class of the proteins. The different arrow shapes represent different types of interactions. Edges are displayed with various labels that describe the nature of the relationship between the nodes.

Malignant transformation of thyroid cyst

Table 4A. Upstream regulators predicted to be regulated in different tissues using IPA software

Upstream regulators	Molecular Type	Activation score		Molecules
		PTC vs Benign	Benign vs PTC	
PD98059	chemical-kinase inhibitor	-2.213	2.213	ANXA1, APOA1, CTSB, SELENBP1, SERPINA1
STAT3	transcription regulator	-1.981	2.207	CTSB, FGB, FGG, HP, PHB, SERPINA1
L-triiodothyronine	chemical-endogenous mammalian	-1.732	1.732	APOA1, HP, PRDX2, PRDX3
MYC	transcription regulator	-1.732	1.732	CAPZB, CTSB, PHB, PRDX2, PRDX3, SERPINA1
TP53	transcription regulator	-1.504	1.504	ALDH9A1, ANXA1, ANXA3, APOA1, CTSB, PRDX2, PRDX3
IL6	cytokine	-1.341	1.353	ANXA1, APOA1, FGB, FGG, HP, PHB, SERPINA1
fenofibrate	chemical drug	1.964	-1.964	APOA1, FGB, FGG, HP
PPARA	ligand-dependant nuclear receptor	1.291	-1.291	ALDH9A1, APOA1, ATP5B, FGB, FGG, SELENBP1
HRAS	enzyme	1	-1	ANXA1, CTSB, HP, PHB
D-glucose	chemical drug	1	-1	ACTG1, ANXA3, ATP5B, CTSB
Nitrofurantoin	chemical-endogenous mammalian	0.816	-0.816	ACTG1, CTSB, FGB, PRDX2, SELENBP1, SERPINA1

For the diseases and functions analyses, benign cold thyroid nodule was the most relevant disease based on the data set with a *p*-value of less than 5.28×10^{-07} . “Metabolism of carbohydrate”, “synthesis of lipid” and “metabolism of protein” were likely to be activated in the PTC tissue. However, “necrosis of epithelial tissue”, “apoptosis”, “cell death” and “necrosis” were likely to be inhibited in the benign tissue whilst “proliferation of cell” was likely to be activated (**Table 4B**).

In addition, seven molecules namely, ANXA1, APOA1, HP, PHB, PRDX2, PRDX3, SERPINA1, are apparently related to “free radical scavenging” including two potent scavengers of H_2O_2 namely PRDX2 and PRDX3, which are also an indication of oxidative stress (**Table 4C**).

Quantitative western blot analysis of STAT3 phosphorylation

Western blot analysis of pY-STAT3 showed presence of two distinct 75 kDa (predicted molecular weight: 88 kDa) and 28 kDa bands and one faint 67 kDa band in the benign cyst, whilst only the 75 and 67 kDa bands were detected in the PTC tissue. A distinct 42 kDa band which corresponds to beta-actin was observed in both tissues (**Figure 5A**). Densitometric evaluation of the blots using Image-J algorithm showed similar total expression of pY-STAT3 in both the benign and PTC tissues. However, the 28 kDa pY-STAT3 fragment, which was termed STAT3 ϵ in the present study, was only expressed in the benign tissue. In contrast, the levels of the 75 and 67 kDa pY-STAT3 proteins found in the PTC tissue appeared 3- and 5-folds higher respec-

tively, compared to the benign tissue. The three 75, 67 and 28 kDa variants of pY-STAT3 were expressed in ratio of 8:1:18 in the benign tissue, while the ratio of the 75 to 67 kDa pY-STAT3 variants was 5:1 in the malignant tissue (**Figure 5B**).

Absence of novel alternatively-spliced STAT3 mRNA

Reverse transcription polymerase chain reaction (RT-PCR) of tcRNA of both tissues did not detect any novel STAT3 mRNA isoform.

Discussion

The concurrent presence of a benign thyroid cyst and PTC in a single patient provided an avenue for us to study the difference between the two tissues and speculate transitional changes that might have occurred during malignancy. In the present study, we demonstrated *BRAF*^{V600E} mutation in the PTC tissue of the patient and further showed the loss of expression of *TG* and *NIS*, and reduced expression of *TPO*. This is nothing new as decreased or loss of expression of *TG*, *NIS* and *TPO* genes due to continued activation of the mitogen-activated protein kinase (MAPK) pathway caused by 1799T>A (p.V600E) mutation in the *BRAF* oncogene often being reported in cases of PTC [27-29]. However, much to our surprise, *NIS* expression was also not detected in the benign cyst of the same patient which was shown not to have the *BRAF*^{V600E} mutation. In this benign tissue, the expression of *TG* and *BRAF* was also found to be highly active whilst *TPO* appeared to be markedly reduced.

Malignant transformation of thyroid cyst

Table 4B. Prediction of disease or function annotation in different tissues using IPA software

Categories	Disease or function annotation	Activation score		Molecules
		PTC vs Benign	Benign vs PTC	
Cell death and survival	necrosis of epithelial tissue	1.969	-1.969	CTSB, PRDX2, PRDX3, SERPINA1
	apoptosis	1.654	-1.654	ANXA1, APOA1, CTSB, GNB2, PHB, PRDX2, PRDX3, SELENBP1, SERPINA1
	cell death	1.43 (*1.927)	-1.43 (*-1.927)	ANXA1, APOA1, *BRAF, CTSB, CNB2, PHB, PRDX2, PRDX3, SELENBP1, SERPINA1
	necrosis	1.298	-1.298	ANXA1, APOA1, CTSB, GNB2, PHB, PRDX2, PRDX3, SERPINA1
Cellular growth and proliferation	Proliferation of cell	*-1.937	*1.937	ACTG1, ANXA1, APOA1, ATP5B, BRAF, CTSB, GNB1, PHB, PRDX2, PRDX3, PSMC2, SELENBP1, SERPINA1, *TG, *TPO, *TSHR
Cancer, organismal injury and abnormalities	growth of tumour	*-1.487	*1.487	ANXA1, APOA1, *BRAF, CTSB, PHB, *TG
Carbohydrate metabolism	metabolism of carbohydrate	1.982	-1.982	APOA1, CTSB, GNB1, PRDX2
Lipid metabolism, small molecule	synthesis of lipid	1.673	-1.673	ANXA1, APOA1, PHB, PRDX2, SERPINA1
Protein synthesis	metabolism of protein	1.103	-1.103	ANXA1, APEH, APOA1, CTSB, PSMC2, SERPINA1

*from real-time PCR data.

Malignant transformation of thyroid cyst

Table 4C. Involvement of the seven identified proteins in the free radical scavenging activity

Categories	Functions Annotation	P-Value	Molecules
Free Radical Scavenging	metabolism of reactive oxygen species	2.12E-06	ANXA1, APOA1, HP, PHB, *PRDX2, *PRDX3, SERPINA1
Free Radical Scavenging	synthesis of reactive oxygen species	2.49E-05	ANXA1, APOA1, HP, PHB, *PRDX2, SERPINA1
Free Radical Scavenging	reduction of hydrogen peroxide	4.55E-05	*PRDX2, *PRDX3
Free Radical Scavenging	reduction of monohydroperoxy-linoleic acid	3.10E-03	*PRDX2
Free Radical Scavenging	metabolite removal of superoxide	1.03E-02	*PRDX2

*An indication of oxidative stress level.

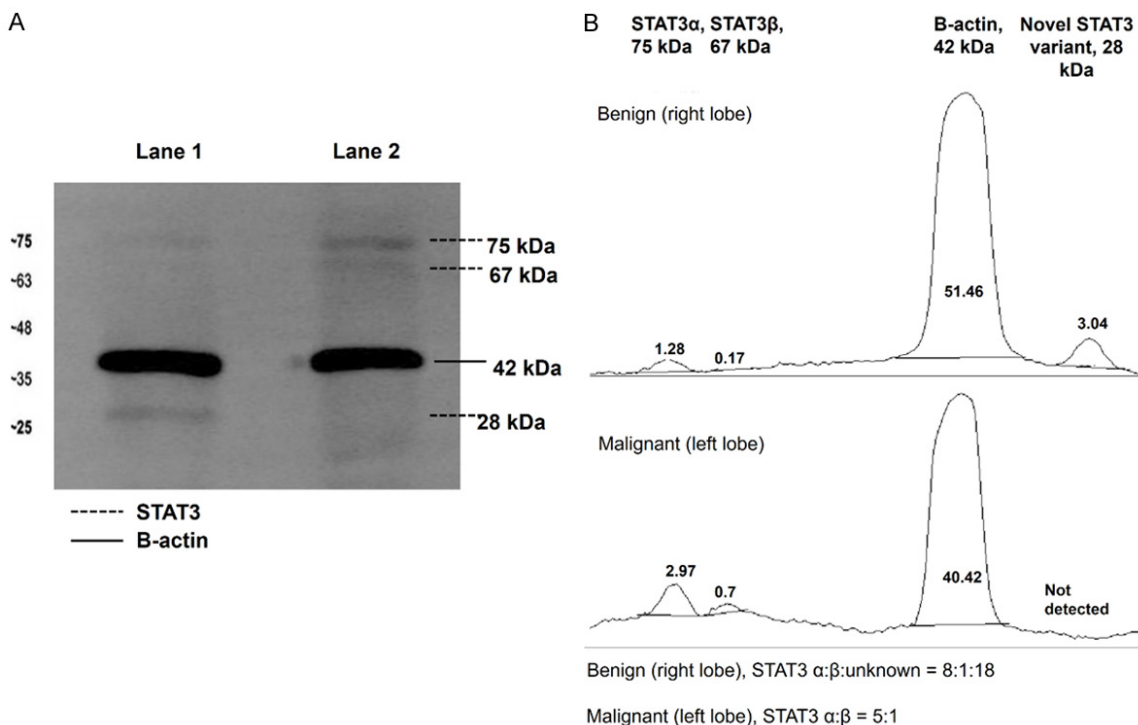


Figure 5. Western blot and Image-J densitometric analyses. Thyroid tissue protein samples were first tested with anti-pYSTAT3 antibody followed by anti- β actin antibody (loading control). Equal amount of microsomal protein (20 μ g) for each sample (100 ng for the positive control) was used. Representative western blot gel picture: Lane 1: benign cyst protein sample; lane 2: PTC protein sample (A). Image-J densitometric quantification of pY-STAT3 isoforms and β actin in the benign cyst and PTC samples (B).

Hydrogen peroxide (H_2O_2) is a reactive oxygen species (ROS) consistently generated during stimulation of the thyroid cells by TSH, and it is a substrate of TPO in the iodination of TG and synthesis of thyroid hormones [30]. In contrast to the decreased expression of TPO, we further noticed that the TSH receptor (TSHR), which is regulated by TSH, was positively expressed in the benign tissue of the patient when compared to three BRAF^{V600E} mutation-free control tissues. The persistent stimulation of TSH under the situation when TPO was not active may have created an H_2O_2 -rich environment in

the benign tissue and caused oxidative stress to the cells. Such a condition may have led to upregulation of TG, which was also observed in the benign cyst in our study, as TG is known to act as a strong suppressor for H_2O_2 production [31]. Our speculation of increased H_2O_2 in the benign cyst receives further support from the findings of relatively higher abundances of PRDX2 and PRDX3 which are potent scavengers of H_2O_2 [32, 33], and altered expression of other ROS or antioxidant defence mechanisms-related proteins when the tissue was subjected to proteomics analysis (Table 4C). All these pro-

Malignant transformation of thyroid cyst

teins were likely to have been generated in response to the increased levels of H_2O_2 in the benign tissue.

Excessive ROS can cause cellular injury and mediate peroxidation of lipids, oxidation of proteins, damage to nucleic acids, enzyme inhibition and apoptosis of cells. Survival of the host depends largely on the ability of cells to handle oxidative insults, either through adaptation, resistance of stress and repair or removal of damaged molecules or cells [34, 35]. When IPA was performed based on proteins that were detected to be differentially expressed between the benign thyroid cyst and PTC tissue, we found that the “acute phase response signalling” was activated in the benign cyst. The concurrent involvement of “coagulation system”, “extrinsic prothrombin activation pathway”, and “intrinsic prothrombin activation pathway” in the same tissue implies injury and/or inflammation, and has often been associated with pathogenesis of various cancers [36]. However, the exact signalling mechanism that links oxidative stress with chronic inflammation as well as cancer remains inconclusive [37] even though they are known to be closely related. A recent study has shown that the release of PRDX2 may function as an inflammatory mediator by triggering macrophages to produce tumour necrosis factor (TNF- α) [38], whilst others postulated involvement of H_2O_2 insults in the tissue which could induce the production of interleukin-6 (IL-6) [39, 40]. In any case, TNF- α and IL-6 are both major inflammatory cytokines involved in cancer-related inflammation, which are under the control of transcription factors, NF- κ B and STAT3 [41]. Recently, the association of H_2O_2 with STAT3 signalling was also unveiled when Sobotta *et al.* demonstrated the modulation of cytokine-induced STAT3 signalling by the expression of PRDX2 which functions as a H_2O_2 signal receptor and transmitter in transcription factor redox regulation [42].

The roles of STAT3 in tumorigenesis were surrounded by controversies. Whilst some studies showed that pY-STAT3 can promote tumorigenesis [43-45] and considered it as a product of an oncogene [46], others demonstrated that the protein inhibited growth of tumour and induced cell apoptosis [47, 48]. More recently, a 67 kDa isoform of STAT3, the STAT3 β , has been suggested to act as a dominant negative factor to STAT3 α (75 kDa) and contributed to

the opposing function of STAT3 [49]. Consistent with this view, a malignant tissue which showed strong activation levels of STAT3 β has been shown to have higher rates of cell necrosis and apoptosis than that of the benign cyst. In our study, however, a 28 kDa fragment of STAT3 with at least 2 fold higher levels than STAT3 α , was instead detected as the main pY-STAT3 isoform in the benign cyst. The fragment, which we termed STAT3 ϵ , was not detected in the PTC tissue of the same patient. This, together with our western blot results which showed similar amounts of pY-STAT3 in both the benign cyst and PTC tissues of our patient implicate the role of STAT3 ϵ in maintaining cell survival and higher proliferation rates in the benign cyst. This hypothesis was further strengthened when IPA predicted that STAT3 and MYC, a proto-oncogene that is a downstream target for many signals such as MAPK and STAT3 pathways and known to induce cell proliferation, reduce apoptosis and promote tumour progression [50], were likely to be activated in the benign cyst. MYC was estimated to have contributed to cause at least 40% of tumours [51]. In spite that it is known to be upregulated in PTC [52] as well as many other cancers [53], overexpression of MYC alone is inefficient at causing malignant transformation [54].

On the other hand, our IPA had also predicted that the PTC cells were likely to display inhibition of p53 which functions as a tumour suppressor by preventing cells with mutated or damaged DNA from dividing [55]. Reduced or loss of p53 function is common at a late stage of tumour development [56]. However, Niu *et al.* has successfully restored the expression of p53 by blocking STAT3 in cancer cells, demonstrating involvement of STAT3 in mediating p53 inhibition [56, 57]. Since both tissues in the present study had presented similar amounts of total pY-STAT3, the STAT3 ϵ that was detected in the benign cyst may have interfered with the binding of STAT3 to the p53 promoter, and hence, retained the p53 function that helped prevent/delay the malignant transformation of the cells. In addition, IPA also revealed an increase in glucose and protein metabolisms and production of lipids in the PTC cells. This is in agreement with the fact that cancer cells frequently exhibit specific alterations in their metabolic activity, termed as the Warburg effect, to support its rapid proliferation [58].

Malignant transformation of thyroid cyst

In both the benign cyst and PTC tissues of our patient, it is noteworthy that the deleterious c.353G>A (p.R118Q) mutation of the *TRH* gene that was detected could have affected the qualitative features of TSH and its secretion from the anterior pituitary. The clinical impact of this gene, which was demonstrated in an animal model using *TRH* knockout mice, showed characteristic phenotypes of tertiary hypothyroidism with a slightly elevated but reduced biological activity of serum TSH and mild hypothyroidism [59]. Although the long-term effects of what appeared to be a novel germ-line mutation of the *TRH* gene remain uncertain, the data of our present study when taken together suggests that it may have caused prolonged H₂O₂ insults which resulted in the extreme oxidative stress that interfered with the MAPK and STAT3 pathways, which then led to *BRAF*^{V600E} mutation and the consequential loss of function of p53 as well as the altered metabolisms and malignant transformation that occurred in PTC. This is amid evidence of higher likelihood of PTC recurrence in *BRAF*^{V600E}-positive compared to *BRAF*^{V600E}-negative patients [60]. Whether the genetic alteration was indeed the predisposing factor that led to the described hypothetical consequential molecular changes and the development of neoplastic thyroid lesions as in our patient is certainly a subject for future investigations.

Acknowledgements

This study was supported financially by grants from the Ministry of Higher Education, Malaysia (H-20001-00-E000009 and FP034-2014A). Written informed consent was obtained from the patient for publication of this Case report and any accompanying images. A copy of the written consent is available for review by the Editor-in-Chief of this journal.

Disclosure of conflict of interest

None.

Authors' contribution

CCL conceived of the study, participated in its design, carried out a major part of molecular studies and data analyses, and drafted the manuscript. MIA participated in the 2-DE analysis. SMJ conceived of the study, participated in its design and was involved in the data analyses. KLN involved in the specimen collection process and contributed the clinical data of the

patient. SYW participated in the Western blot analysis. NSFR participated in specimen processing procedure. OHH conceived of the study, participated in its design and coordination, helped to analyze the data and critically revised the manuscript. All authors read and approved the final manuscript.

Address correspondence to: Dr. Onn Haji Hashim, Department of Molecular Medicine, Faculty of Medicine, University of Malaya, 50603, Lembah Pantai, Kuala Lumpur, Malaysia. Tel: +603-7967 4906; Fax: +603-7967 4957; E-mail: onnhashim@um.edu.my

References

- [1] Brander A, Viikinkoski P, Nickels J and Kivisaari L. Thyroid gland: US screening in a random adult population. *Radiology* 1991; 181: 683-687.
- [2] Wienke JR, Chong WK, Fielding JR, Zou KH and Mittelstaedt CA. Sonographic features of benign thyroid nodules: interobserver reliability and overlap with malignancy. *J Ultrasound Med* 2003; 22: 1027-1031.
- [3] Tan GH and Gharib H. Thyroid incidentalomas: management approaches to nonpalpable nodules discovered incidentally on thyroid imaging. *Ann Intern Med* 1997; 126: 226-231.
- [4] Ezzat S, Sarti DA, Cain DR and Braunstein GD. Thyroid incidentalomas. Prevalence by palpation and ultrasonography. *Arch Intern Med* 1994; 154: 1838-1840.
- [5] Laurberg P, Pedersen KM, Hreidarsson A, Sigfusson N, Iversen E and Knudsen PR. Iodine intake and the pattern of thyroid disorders: a comparative epidemiological study of thyroid abnormalities in the elderly in Iceland and in Jutland, Denmark. *J Clin Endocrinol Metab* 1998; 83: 765-769.
- [6] Vanderpump MP. The epidemiology of thyroid disease. *Br Med Bull* 2011; 99: 39-51.
- [7] Guth S, Theune U, Aberle J, Galach A and Bamberger CM. Very high prevalence of thyroid nodules detected by high frequency (13 MHz) ultrasound examination. *Eur J Clin Invest* 2009; 39: 699-706.
- [8] Diez JJ. Goiter in adult patients aged 55 years and older: etiology and clinical features in 634 patients. *J Gerontol A Biol Sci Med Sci* 2005; 60: 920-923.
- [9] Bonert V and Friedman TC. The thyroid gland. In: Andreoli TE, Carpenter CCJ, Cecil RL, editors. *Andreoli and Carpenter's Cecil essentials of medicine*. 7th edition. Philadelphia: Saunders; 2007. pp. 593-602.
- [10] Smith TJ. Neck and Thyroid Examination. In: Walker HK, Hall WD, Hurst JW, editors. *Clinical*

Malignant transformation of thyroid cyst

- Methods: The History, Physical, and Laboratory Examinations. 3rd edition. Boston: 1990.
- [11] Hegedus L, Bonnema SJ and Bennedbaek FN. Management of simple nodular goiter: current status and future perspectives. *Endocr Rev* 2003; 24: 102-132.
- [12] Gandolfi PP, Frisina A, Raffa M, Renda F, Rocchetti O, Ruggeri C and Tombolini A. The incidence of thyroid carcinoma in multinodular goiter: retrospective analysis. *Acta Biomed* 2004; 75: 114-117.
- [13] Cole WH. Incidence of carcinoma of the thyroid in nodular goiter. *Semin Surg Oncol* 1991; 7: 61-63.
- [14] Sachmechi I, Miller E, Varatharajah R, Chernys A, Carroll Z, Kissin E and Rosner F. Thyroid carcinoma in single cold nodules and in cold nodules of multinodular goiters. *Endocr Pract* 2000; 6: 5-7.
- [15] Smith JJ, Chen X, Schneider DF, Broome JT, Sippel RS, Chen H and Solorzano CC. There is a High Rate of Incidental Thyroid Cancer in Surgical Series of Toxic and Nontoxic Multinodular Goiter. *Clin Thyroidol* 2013; 25: 168-169.
- [16] Othman NH, Omar E and Naing NN. Spectrum of thyroid lesions in hospital Universiti Sains Malaysia over 11years and a review of thyroid cancers in Malaysia. *Asian Pac J Cancer Prev* 2009; 10: 87-90.
- [17] Li H and Durbin R. Fast and accurate long-read alignment with Burrows-Wheeler transform. *Bioinformatics* 2010; 26: 589-595.
- [18] Li R, Li Y, Fang X, Yang H, Wang J, Kristiansen K and Wang J. SNP detection for massively parallel whole-genome resequencing. *Genome Res* 2009; 19: 1124-1132.
- [19] Li H, Handsaker B, Wysoker A, Fennell T, Ruan J, Homer N, Marth G, Abecasis G, Durbin R; 1000 Genome Project Data Processing Subgroup. The Sequence Alignment/Map format and SAMtools. *Bioinformatics* 2009; 25: 2078-2079.
- [20] Lee CC, Harun F, Jalaludin MY, Heh CH, Othman R and Mat Junit S. A Novel, Homozygous c.1502T>G (p.Val501Gly) Mutation in the Thyroid peroxidase Gene in Malaysian Sisters with Congenital Hypothyroidism and Multinodular Goiter. *Int J Endocrinol* 2013; 2013: 987186.
- [21] Shevchenko A, Tomas H, Havlis J, Olsen JV and Mann M. In-gel digestion for mass spectrometric characterization of proteins and proteomes. *Nat Protoc* 2006; 1: 2856-2860.
- [22] Wu J, Patmore DM, Jousma E, Eaves DW, Breving K, Patel AV, Schwartz EB, Fuchs JR, Cripe TP, Stemmer-Rachamimov AO and Ratner N. EGFR-STAT3 signaling promotes formation of malignant peripheral nerve sheath tumors. *Oncogene* 2014; 33: 173-180.
- [23] Shimko MJ, Zaccone EJ, Thompson JA, Schwegler-Berry D, Kashon ML and Fedan JS. Nerve growth factor reduces amiloride-sensitive Na⁺ transport in human airway epithelial cells. *Physiol Rep* 2014; 2.
- [24] Lee CC, Harun F, Jalaludin MY, Lim CY, Ng KL and Mat Junit S. Functional analyses of C.2268dup in thyroid peroxidase gene associated with goitrous congenital hypothyroidism. *Biomed Res Int* 2014; 2014: 370538.
- [25] Wong LP, Ong RT, Poh WT, Liu X, Chen P, Li R, Lam KK, Pillai NE, Sim KS, Xu H, Sim NL, Teo SM, Foo JN, Tan LW, Lim Y, Koo SH, Gan LS, Cheng CY, Wee S, Yap EP, Ng PC, Lim WY, Soong R, Wenk MR, Aung T, Wong TY, Khor CC, Little P, Chia KS and Teo YY. Deep whole-genome sequencing of 100 southeast Asian Malays. *Am J Hum Genet* 2013; 92: 52-66.
- [26] 1000 Genomes Project Consortium, Abecasis GR, Altshuler D, Auton A, Brooks LD, Durbin RM, Gibbs RA, Hurles ME and McVean GA. A map of human genome variation from population-scale sequencing. *Nature* 2010; 467: 1061-1073.
- [27] Durante C, Puxeddu E, Ferretti E, Morisi R, Moretti S, Bruno R, Barbi F, Avenia N, Scipioni A, Verrienti A, Tosi E, Cavaliere A, Gulino A, Filetti S and Russo D. BRAF mutations in papillary thyroid carcinomas inhibit genes involved in iodine metabolism. *J Clin Endocrinol Metab* 2007; 92: 2840-2843.
- [28] Romei C, Ciampi R, Faviana P, Agate L, Molinaro E, Bottici V, Basolo F, Miccoli P, Pacini F, Pinchera A and Elisei R. BRAFV600E mutation, but not RET/PTC rearrangements, is correlated with a lower expression of both thyroperoxidase and sodium iodide symporter genes in papillary thyroid cancer. *Endocr Relat Cancer* 2008; 15: 511-520.
- [29] Espadinha C, Santos JR, Sobrinho LG and Bugalho MJ. Expression of iodine metabolism genes in human thyroid tissues: evidence for age and BRAFV600E mutation dependency. *Clin Endocrinol (Oxf)* 2009; 70: 629-635.
- [30] Corvilain B, van Sande J, Laurent E and Dumont JE. The H₂O₂-generating system modulates protein iodination and the activity of the pentose phosphate pathway in dog thyroid. *Endocrinology* 1991; 128: 779-785.
- [31] Yoshihara A, Hara T, Kawashima A, Akama T, Tanigawa K, Wu H, Sue M, Ishido Y, Hiroi N, Ishii N, Yoshino G and Suzuki K. Regulation of dual oxidase expression and H₂O₂ production by thyroglobulin. *Thyroid* 2012; 22: 1054-1062.
- [32] Kang SW, Chae HZ, Seo MS, Kim K, Baines IC and Rhee SG. Mammalian peroxiredoxin isoforms can reduce hydrogen peroxide generated in response to growth factors and tumor

Malignant transformation of thyroid cyst

- necrosis factor- α . *J Biol Chem* 1998; 273: 6297-6302.
- [33] Kim H, Lee TH, Park ES, Suh JM, Park SJ, Chung HK, Kwon OY, Kim YK, Ro HK and Shong M. Role of peroxiredoxins in regulating intracellular hydrogen peroxide and hydrogen peroxide-induced apoptosis in thyroid cells. *J Biol Chem* 2000; 275: 18266-18270.
- [34] Fulda S, Gorman AM, Hori O and Samali A. Cellular stress responses: cell survival and cell death. *Int J Cell Biol* 2010; 2010: 214074.
- [35] Sharma P, Jha AB, Dubey RS and Pessarakli M. Reactive Oxygen Species, Oxidative Damage, and Antioxidative Defense Mechanism in Plants under Stressful Conditions. *Journal of Botany* 2012; 2012.
- [36] Hanahan D and Weinberg RA. Hallmarks of cancer: the next generation. *Cell* 2011; 144: 646-674.
- [37] Reuter S, Gupta SC, Chaturvedi MM and Aggarwal BB. Oxidative stress, inflammation, and cancer: how are they linked? *Free Radic Biol Med* 2010; 49: 1603-1616.
- [38] Salzano S, Checconi P, Hanschmann EM, Lillig CH, Bowler LD, Chan P, Vaudry D, Mengozzi M, Coppo L, Sacre S, Atkuri KR, Sahaf B, Herzenberg LA, Herzenberg LA, Mullen L and Ghezzi P. Linkage of inflammation and oxidative stress via release of glutathionylated peroxiredoxin-2, which acts as a danger signal. *Proc Natl Acad Sci U S A* 2014; 111: 12157-12162.
- [39] Wu WC, Hu DN, Gao HX, Chen M, Wang D, Rosen R and McCormick SA. Subtoxic levels hydrogen peroxide-induced production of interleukin-6 by retinal pigment epithelial cells. *Mol Vis* 2010; 16: 1864-1873.
- [40] Colston JT, Chandrasekar B and Freeman GL. A novel peroxide-induced calcium transient regulates interleukin-6 expression in cardiac-derived fibroblasts. *J Biol Chem* 2002; 277: 23477-23483.
- [41] Mantovani A, Allavena P, Sica A and Balkwill F. Cancer-related inflammation. *Nature* 2008; 454: 436-444.
- [42] Sobotta MC, Liou W, Stocker S, Talwar D, Oehler M, Ruppert T, Scharf AN and Dick TP. Peroxiredoxin-2 and STAT3 form a redox relay for H2O2 signaling. *Nat Chem Biol* 2015; 11: 64-70.
- [43] Tye H, Kennedy CL, Najdovska M, McLeod L, McCormack W, Hughes N, Dev A, Sievert W, Ooi CH, Ishikawa TO, Oshima H, Bhathal PS, Parker AE, Oshima M, Tan P and Jenkins BJ. STAT3-driven upregulation of TLR2 promotes gastric tumorigenesis independent of tumor inflammation. *Cancer Cell* 2012; 22: 466-478.
- [44] Azare J, Leslie K, Al-Ahmadie H, Gerald W, Weinreb PH, Violette SM and Bromberg J. Constitutively activated Stat3 induces tumorigenesis and enhances cell motility of prostate epithelial cells through integrin beta 6. *Mol Cell Biol* 2007; 27: 4444-4453.
- [45] Diaz N, Minton S, Cox C, Bowman T, Gritsko T, Garcia R, Eweis I, Wloch M, Livingston S, Seijo E, Cantor A, Lee JH, Beam CA, Sullivan D, Jove R and Muro-Cacho CA. Activation of stat3 in primary tumors from high-risk breast cancer patients is associated with elevated levels of activated SRC and survivin expression. *Clin Cancer Res* 2006; 12: 20-28.
- [46] Bromberg JF, Wrzeszczynska MH, Devgan G, Zhao Y, Pestell RG, Albanese C and Darnell JE Jr. Stat3 as an oncogene. *Cell* 1999; 98: 295-303.
- [47] de la Iglesia N, Konopka G, Puram SV, Chan JA, Bachoo RM, You MJ, Levy DE, Depinho RA and Bonni A. Identification of a PTEN-regulated STAT3 brain tumor suppressor pathway. *Genes Dev* 2008; 22: 449-462.
- [48] Lee J, Kim JC, Lee SE, Quinley C, Kim H, Herdman S, Corr M and Raz E. Signal transducer and activator of transcription 3 (STAT3) protein suppresses adenoma-to-carcinoma transition in Apcmin/+ mice via regulation of Snail-1 (SNAIL) protein stability. *J Biol Chem* 2012; 287: 18182-18189.
- [49] Zhang HF and Lai R. STAT3 in Cancer-Friend or Foe? *Cancers (Basel)* 2014; 6: 1408-1440.
- [50] Dang CV. MYC, metabolism, cell growth, and tumorigenesis. *Cold Spring Harb Perspect Med* 2013; 3.
- [51] Miller DM, Thomas SD, Islam A, Muench D and Sedoris K. c-Myc and cancer metabolism. *Clin Cancer Res* 2012; 18: 5546-5553.
- [52] Zhu X, Zhao L, Park JW, Willingham MC and Cheng SY. Synergistic signaling of KRAS and thyroid hormone receptor beta mutants promotes undifferentiated thyroid cancer through MYC up-regulation. *Neoplasia* 2014; 16: 757-769.
- [53] Chen BJ, Wu YL, Tanaka Y and Zhang W. Small molecules targeting c-Myc oncogene: promising anti-cancer therapeutics. *Int J Biol Sci* 2014; 10: 1084-1096.
- [54] Loosveld M, Bonnet M, Gon S, Montpellier B, Quilichini B, Navarro JM, Crouzet T, Goujart MA, Chasson L, Morgado E, Picard C, Hernandez L, Fossat C, Gabert J, Michel G, Nadel B and Payet-Bornet D. MYC fails to efficiently shape malignant transformation in T-cell acute lymphoblastic leukemia. *Genes Chromosomes Cancer* 2014; 53: 52-66.
- [55] Zilfou JT and Lowe SW. Tumor suppressive functions of p53. *Cold Spring Harb Perspect Biol* 2009; 1: a001883.

Malignant transformation of thyroid cyst

- [56] Muller PA, Vousden KH and Norman JC. p53 and its mutants in tumor cell migration and invasion. *J Cell Biol* 2011; 192: 209-218.
- [57] Niu G, Wright KL, Ma Y, Wright GM, Huang M, Irby R, Briggs J, Karras J, Cress WD, Pardoll D, Jove R, Chen J and Yu H. Role of Stat3 in regulating p53 expression and function. *Mol Cell Biol* 2005; 25: 7432-7440.
- [58] Vander Heiden MG, Cantley LC and Thompson CB. Understanding the Warburg effect: the metabolic requirements of cell proliferation. *Science* 2009; 324: 1029-1033.
- [59] Yamada M and Mori M. Mechanisms related to the pathophysiology and management of central hypothyroidism. *Nat Clin Pract Endocrinol Metab* 2008; 4: 683-694.
- [60] Xing M, Alzahrani AS, Carson KA, Shong YK, Kim TY, Viola D, Elisei R, Bendlova B, Yip L, Mian C, Vianello F, Tuttle RM, Robenshtok E, Fagin JA, Puxeddu E, Fugazzola L, Czarniecka A, Jarzab B, O'Neill CJ, Sywak MS, Lam AK, Riesco-Eizaguirre G, Santisteban P, Nakayama H, Clifton-Bligh R, Tallini G, Holt EH and Sykorova V. Association between BRAF V600E mutation and recurrence of papillary thyroid cancer. *J Clin Oncol* 2015; 33: 42-50.